Preprint Title	Synthesis of aminonaphthoquinone derivatives with Ceric Ammonium Nitrate (CAN) as a catalyst: NMR characterization and *in silico* reaction mechanism
Authors	Jhoan H. Piermattey, Jhon Zapata-Rivera, Juan Oviedo, Ricardo Gaitan and Harold Gomez
Publication Date	09 Nov 2020
Article Type	Full Research Paper
Supporting Information File 1	S1.pdf; 61.5 KB
Supporting Information File 2	S2.pdf; 709.2 KB
Supporting Information File 3	S3.pdf; 737.9 KB
Supporting Information File 4	S4.pdf; 654.8 KB
ORCID® iDs	Jhoan H. Piermattey - https://orcid.org/0000-0002-7319-4577; Jhon Zapata-Rivera - https://orcid.org/0000-0001-8329-3571; Harold Gomez - https://orcid.org/0000-0003-3412-8881

Synthesis of aminonaphthoquinone derivatives with Ceric Ammonium Nitrate (CAN) as a catalyst: NMR characterization and *in silico* reaction mechanism

Jhoan H. Piermattey*‡[1], Jhon Zapata-Rivera‡[2], Juan Oviedo‡[1], Ricardo Gaitan†, Harold Gómez[3]

[1]Natural Products Group, Faculty of Pharmaceutical Sciences, University of Cartagena, Carrera 50 No. 29-11, 130014, Cartagena, Colombia.

[2]Molecular Electronic Structure Group, Department of Chemistry, Universidad de los Andes. Cra 1 No. 18A – 12, 111711, Bogotá. Colombia.

[3]Research group in Medicinal Organic Chemistry, Faculty of Pharmaceutical Sciences, University of Cartagena, Carrera 50 No. 29-11, 130014, Cartagena, Colombia.

Email: Jhoan H. Piermattey – jpiermatteyd@unicartagena.edu.co

* Corresponding author

‡ Equal contributors

†Deceased

Abstract

Three different aminonaphthoquinones of great interest in medicinal chemistry due to their diverse biological activities were more efficiently synthesized and characterized starting from naphthoquinones with hydrazoic acid in the presence of ceric ammonium nitrate (CAN). We have previously reported a highly time demand synthesis of 2-amino-1,4-naphthoquinone and 2-amino-3-methyl-1,4-naphthoquinone in the absence of the CAN catalyst. In the current study, we have also obtained 3-amino-5-hydroxy-

1,4-naphthoquinone and reduced all reaction times in the presence of CAN as a catalyst. Reaction rates have been increased to circa three times their original times. All aminonaphthoquinones have been characterized by NMR, vibrational, and chromatographic techniques. Additionally, we have proposed a reaction mechanism for the amination of naphthoquinone derivatives in an acid medium, based on in-depth DFT calculations.

Keywords

Amination; Ceric Ammonium; Aminonaphthoquinones; Reaction Mechanism; DFT calculations.

Introduction

Naphthoquinones are aromatic compounds very abundant in nature, distributed in higher plants, bacteria, fungi, arthropods, and individual representatives of the animal kingdom [1–3]. Aminonaphthoquinones are of great interest in medicinal chemistry due to the variety of biological activities they present as cytotoxic, antimalarial, antifungal, antibacterial, anti-inflammatory, and antitumor agents [4–10]. Since naphthoquinones mainly present nucleophilic addition and substitution reactions, their amination reactions occur in an acid medium where the oxygen of a ketone group of the molecule acts as a Lewis base causing the delocalization of π electrons present in the quinone nucleus, where nucleophilic agents like amino groups can attack [11] (Scheme 1).

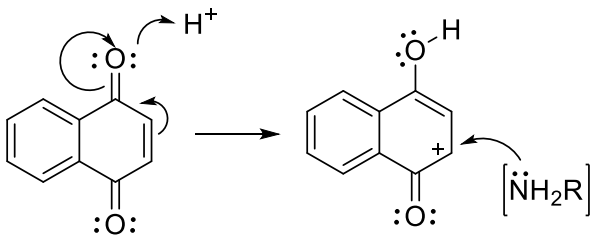

Scheme 1: Electron delocalization of 1,4-naphthoquinone in acid medium.

The amination of 1,4-naphthoquinone derivatives is an essential step in the synthetic pathway of more complex derivatives such as indolequinones [12–15]. The synthesis of aminonaphthoquinones is possible by reacting 1,4-naphthoquinone derivatives with nucleophiles agents such as hydroxylamines, gaseous ammonia, sodium nitrite with subsequent reduction, primary amines, and hydrazoic acid [11]. The reaction between quinone derivatives and hydrazoic acid have been widely studied in terms of reaction conditions and reaction mechanism [16,17]. However, concerning to aminonaphthoquinones, the evaluation of more efficient routes of synthesis, as well as an in-depth study of the formation mechanism, to the best of our knowledge has not been reported.

We have previously reported the synthesis of 2-amino-1,4-naphthoquinone and 2-amino-3-methyl-1,4-naphthoquinone by the reaction between hydrazoic acid (formed in situ) and 1,4- naphthoquinone and 2-methyl-1,4-naphthoquinone, respectively [2, 18]. In this work, it has been studied the effect of the ceric ammonium nitrate (CAN) catalyst in this type of amination reaction. The amination of 1,4-naphthoquinone was first accomplished with hydrazoic acid and different CAN concentrations as a reaction catalyst. Subsequently, the compounds 2-amino-1,4-naphthoquinones, 2-amino-3-methyl-1,4-naphthoquinone, and 3-amino-5-hydroxy-1,4-naphthoquinone were synthesized with a molar ratio of 1:1 (starting compound/catalyst). The results obtained from the reaction conditions were compared and discussed respect to those obtained in the absence of catalyst reported by our research group and other authors [2,18]. Additionally, we carried out an *in silico* study of the more favorable reaction mechanism of the amination of naphthoquinone derivatives in acidic medium. With the here reported results we want to contribute to the study of the amination reactions of

quinone compounds that lead to more efficient reaction conditions in energy consumption and reaction time.

Results and Discussion

Chemistry

In this study, all amination reactions were carried out in ethanol/water (5:3, v/v) at pH 4. Hydrazoic acid was prepared *in situ*, maintaining a 1:6 molar ratio of starting material/azide of sodium. The reaction temperature was established by starting the experiments at room temperature and 50 ºC if no reaction was observed (Scheme 2). The reaction time was determined by monitoring with thin layer chromatography.

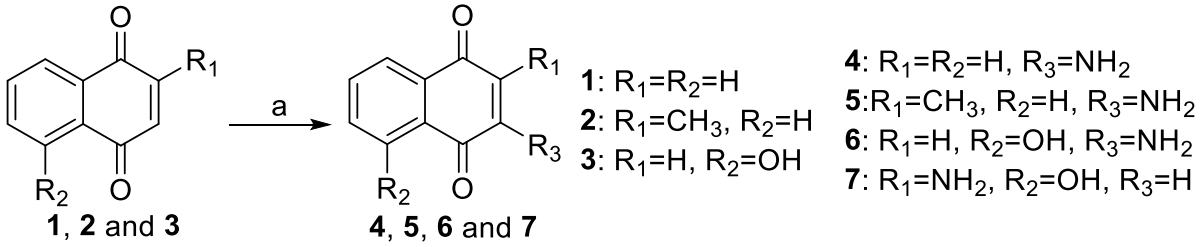

Scheme 2: General synthesis of aminonaphthoquinone derivatives. a) sodium azide, Hydrochloric acid, Ceric ammonium nitrate (CAN).

Initially, to observe the effect of the amount of catalyst in the amination reaction, the synthesis of **4** was carried out by varying the molar proportions of CAN. Table 1 shows the proportions of CAN used and the yields in each reaction (I-IV).

Table 1: Amination reaction yields of 1,4-naphthoquinone with different molar ratios of ceric ammonium nitrate (CAN).

Reaction	**I**	**II**	**III**	**IV**
Molar ratios[a]	1:1	1:2	2:5	1:3
% Yield	48%	37%	21%	8%

[a]Molar ratios are given as **Compound 1:CAN**.

As a result, an inversely proportional relationship between the amount of catalyst and the reaction yield is evident. Cerium has been proposed as a reaction mechanism to act as a Lewis base, binding to one of the carbonyl oxygens of naphthoquinones, triggering a delocalization of electrons that would activate the quinone ring for a nucleophilic attack [19,20]. It is likely that an excess of catalyst in the reaction acts as an oxidizing agent and not as a Lewis base, causing the appearance of unwanted products and a lower yield. This hypothesis is supported by observing the chromatographic profiles made after each reaction, where higher proportions of catalyst generate more complex profiles with higher numbers of spots (Figure S1).

Table 2 shows a comparison of the reaction times and temperatures and the reaction yield in synthesizing aminonaphthoquinones derivatives with/without a catalyst. All amination reactions with CAN showed a reduction in reaction times versus reactions without the catalyst. The coordination bond between the carbonyl oxygen and cerium (IV) may be more stable than that established with the proton of the acidic medium, generating a more favorable chemical balance for the nucleophilic attack of the azide, increasing the kinetics of the reaction.

Table 2: Comparison of the reaction conditions and yield of compounds **4**-**7** with and without the catalyst (CAN).

	With CAN			**Without CAN**			
	Reaction Time (h)	**Temp. of reaction (ºC)**	**% Yield**	**Reaction Time (h)**	**Temp. of reaction (ºC)**	**% Yield**	**Ref**
4	6	rt.	48	16	60	90	[18]
5	16	60	66	36	60	69	[18]
6	15	rt.	35	5	rt	62	[21][b]

7	15	rt.	0[a]	24	rt	20	[22][c]

[a]Not detected by gas chromatography/mass. [b]Amination with hydroxylamine. [c]Direct amination.

On the other hand, it was possible to obtain compounds **4** and **6** at room temperature, indicating a decrease in activation energy when using CAN in the amination reactions. For compound **5**, no change in reaction temperature is observed when CAN is used in the reaction; there is no decrease in the activation energy of this reaction due to the steric effect exerted by the methyl group near the azide attack site. Finally, in the amination reaction of **3**, we expected to obtain a mixture of two isomers, **6** and **7**, but it was only possible to identify compound **6**. The amino group position in compound **6** was assigned by analyzing the HSQC and HMBC spectra (Figure 1). Seemingly the hydrogen bond formed between the hydroxyl group in the C5 position and the C4 carbonyl group limits the interaction of cerium (IV) with the latter, increasing the probability of union with the oxygen of the C1 carbonyl that is free, driving the azide attack at position C3 (Scheme 3). This regioselective nucleophilic attack at the C3 position of compound **3** is observed when amination is carried out with hydroxylamine, obtaining both isomers with a higher yield of compound **6** [21]. On the contrary, when the reaction is accomplished by direct amination with ammonia in methanol, compound **7** is the only product. However, If a methoxy group replaces the hydroxyl at C5, the amination occurs at C3 [22].

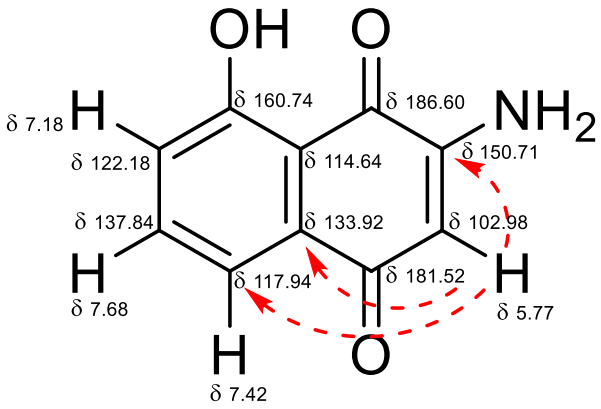

Figure 1: Structural elucidation of 3-amino-5-hydroxy-1,4-naphthoquinone. Chemical shifts in ppm of by NMR are shown for ^{1}H and ^{13}C. Red dashed arrows indicate the interactions of the proton joined to C2 at 5.77 ppm chemical shift with carbons 3, 8, and 9.

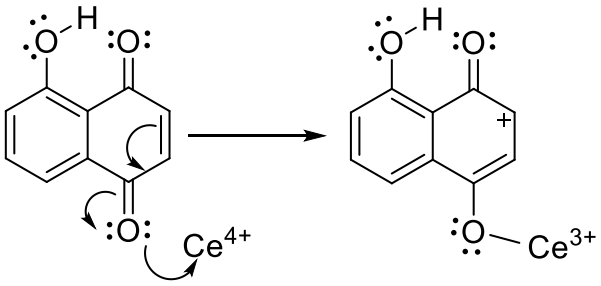

Scheme 3: Proposed reaction mechanism for the regioselective amination of 5-hydroxy-1,4-naphthoquinone mediated by Ce (IV).

Theoretical Reaction Mechanism

Reaction energies and spontaneity

Geometry optimization calculations have been performed on the naphthoquinones (compounds **1**-**3** in Figure 2), as well as on the aminonaphthoquinones of the products (compounds **4**-**6** in Figure 2), in order to estimates the reaction energies by considering $\Delta E = E_{prod} - E_{reac}$. In this expression, E_{reac} and E_{prod} correspond to the sum of the absolute energies of reactants and products. It is worth mentioning that the CAN catalyst effect has not been explored because its action has been demonstrated to be

mostly kinetic. Compounds **1**-**6** have a singlet ground state with an electronic structure characterized by frontier molecular orbitals of π nature mainly located on the naphthalene fragment. The calculated reaction energies (ΔE), including enthalpies (ΔH) and Gibbs free energies (ΔG), are reported in Table 3. The great amplitude and negative sign of the energies (ΔE < -104 kcal·mol^{-1}) indicate the considerable stability of products over to reactants. Similarly, the great exothermicity and spontaneity of the reaction is also confirmed by ΔH < -106 kcal·mol^{-1} and ΔG < -105 kcal·mol^{-1}. These values reveal that the overall amination reaction is thermodynamically irreversible and is in line with a high reaction yield, as observed in the experiments.

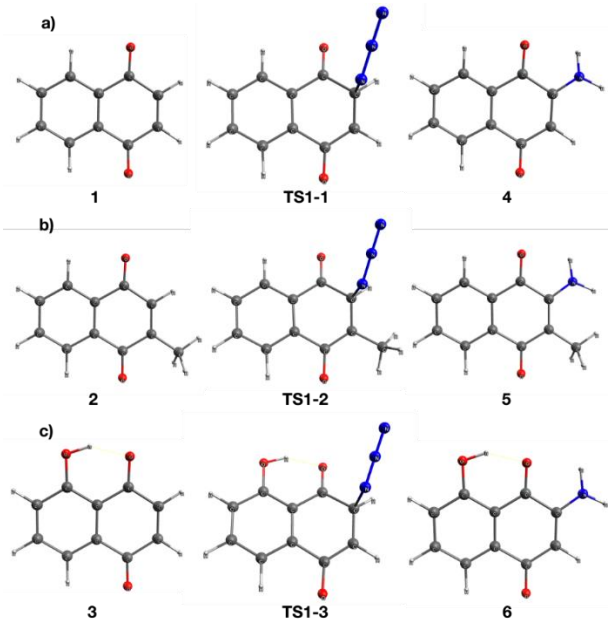

Figure 2: Optimized structures of naphthoquinones **1**-**3**, aminonaphthoquinones **4**-**6**, and their corresponding transition states (TS).

Table 3: The calculated reaction energies (ΔE), enthalpies (ΔH), and Gibbs free energies (ΔG). All values in kcal·mol^{-1}.

	R1	R2	ΔE	ΔH	ΔG
1 to **4**	H	H	-110.45	-111.20	-110.90
2 to **5**	H	CH_3	-104.71	-106.09	-105.17

3 to **6**	OH	H	-110.93	-111.63	-111.15

We have also carried out analytical frequency calculations to perform the theoretical IR spectra of the reactants **1**-**3** and products **4**-**6**. It is worth noting that no negative frequencies were found on the above optimized geometries, indicating that each structure is a global minimum. Table 4 shows the correspondence between some theoretical and experimental characteristic IR bands of the products. In general, the bands are well matched, which supports the prediction ability of the computational method. However, it can be seen that the lower energy, the better match of the bands. The IR spectra of compounds **4**-**6** are comparable to each other, as shown in Figure S2. Three regions are well defined for each aminonaphthoquinone: 1) the low energy bands, below 1500 cm^{-1}, are associated with the twisting and scissoring of the aromatic hydrogens. 2) the bands between the 1500 and 1700 cm^{-1} result from symmetric and asymmetric stretching of the carbons belonging to the aromatic rings. 3) Finally, the high energy bands, above 3500 cm^{-1}, result from symmetric and asymmetric stretching of the hydrogens in the amino group. Notably, compound **3** shows an additional band close to 3000 cm-1, which is associated with the stretching of hydrogen in the alcohol group. The proximity between the calculated and experimental spectra has enabled identifying the isolated products as the here synthesized aminonaphthoquinones (compounds **4**-**6**).

Table 4: Comparison between theoretical and experimental IR bands of the aminonaphthoquinones **4**-**6**. All values in cm^{-1}.

4		**5**		**6**	
ν_{Cal} (cm^{-1})	ν_{Exp} (cm^{-1})	ν_{Cal} (cm^{-1})	ν_{Exp} (cm^{-1})	ν_{Cal} (cm^{-1})	ν_{Exp} (cm^{-1})
291.9		203.7		324.8	
754.0	720.3	429.4	421.4	892.8	825.5
863.1	857.2	749.6	725.1	1254.2	
1006.2	983.5	1033.7	1022.1	1286.0	1265.3

1283.6	1222.7	1246.2	1217.9	1320.9	
1293.5	1269.9	1300.1 1367.7	1270.9 1285.3	1413.6	1379.1
1363.1	1367.3			1429.3	
1393.2		1397.7	1357.7	1493.1	
1424.6		1415.8		1512.8	1454.3
1554.7		1553.8	1576.6	1553.7	
1625.0	1607.4	1624.7		1620.9	
1642.9		1642.7	1623.8	1634.7	
1659.6		1661.3		1661.5	1556.6
1703.6	1686.5	1700.2	1664.3	1675.7	1585.5
1759.4		1750.8		1760.5	1714.7
3560.0	3301.6	3570.0	3343.1	3055.9	2924.1
3692.4	3444.3	3706.1	3455.9	3555.8	3350.0
				3688.5	3394.7

Activation energies and reaction profile

We have also explored different pathways to establish the reaction mechanism of the amination process of compounds **1**-**3**. Geometry optimizations of the stationary points within each reaction have been performed so that, according to reported mechanisms of similar quinones [17], the minimum energy path able to connect **1**-**3** with **4**-**6** would be assessed, respectively. The whole reaction can be understood as a nucleophilic substitution; however, the solved mechanism concern series of reaction steps of nucleophilic addition and elimination that lead to the formation of different reaction intermediates.

Let us explain the reaction mechanism of compounds **1**-**3** as follows: the first stage of the reaction consists of nucleophilic addition of the azido anion that results in the formation of the keto form 2-azidohydroquinone (Int1 in Scheme 4). Some experimental data suggest that this step is the slower, and hence rate limiting step of the reaction [17]. Accordingly, we have searched the corresponding Transition State (TS) to estimates the activation energy for the formation of each aminonaphthoquinone. The optimized geometries of the three TS are depicted in

Figure 2; they have been labeled as TS1-1, TS1-2, and TS1-3 for compounds **1**-**3**, respectively. In all structures, the bonded nitrogen of the azido fragment retains the trigonal planar electron pair arrangement.

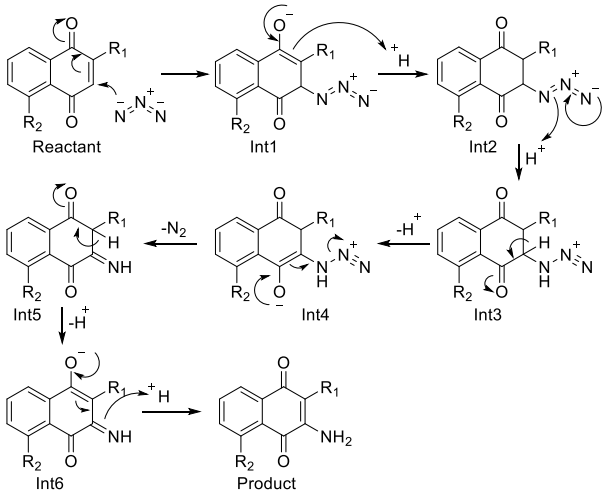

Scheme 4: Proposed reaction mechanism based on the minimum energy path at the B3LYP level of calculation.

Table 5 shows the activation values of the thermodynamical state variables. The reported values indicate that the formation of the azido intermediate is thermodynamically feasible at STP conditions. In compounds **1** and **3**, lower activation energies have been achieved, 1.53 and 0.54 kcal·mol^{-1}, respectively. Instead, in compound **2**, the activation energy is as high as 7.54 kcal·mol^{-1}, which suggests the need to increase the temperature slightly to exceed the activation barrier. In fact, in the synthesis of compound **5** from **2**, a heating up to 60 ºC was required to accomplish the reaction. Once the barrier has been overcome, the azide addition induces the ionization of oxygen of carbonyl group in C1; in consequence, the C-O bond distance rises from 1.2 to 1.4 Å, and Int1 is reached at ca. 0.1 kcal·mol^{-1} below the TS1. The acidic medium of the reaction readily stabilizes this reduced oxygen. From Int1 continues the protonation of C2, leading to the formation of a second intermediate Int2

(Scheme 4). Protonation and deprotonation processes in this kind of system are usually barrierless or with small barriers [23]. Our exploratory calculations in the different protonation and deprotonation steps of this study were consistent with the barrier lower than 0.05 kcal·mol^{-1}, hence their corresponding TSs have been not included in our reaction profiles. In all reactions, the formation of Int2 is stabilized beyond 46 kcal·mol^{-1} (Figure 3) and is accompanied by the deprotonation of oxygen of the carbonyl group in C1. Then, the protonation of nitrogen on C3 leads to the formation of intermediate Int3 at higher energy than Int2. This process weakens the N-N double bond, which elongates from 1.2 to 1.4 Å. Subsequently, the deprotonation of C3 allows the formation of intermediates Int4. The hydrogen cleavage induces the oxygen ionization in C4, and C-O bond length rises from 1.2 up to 1.4 Å. Deionization of oxygen in C4 routes the reaction to forming the most stable intermediate Int5 and the N_2 elimination. This process is carried out via a transition state TS2 with a negligible barrier (lower than 0.01 kcal·mol^{-1}). Later on, the deprotonation of C2 leads to the destabilization of intermediate Int6, where the oxygen in C1 is again ionized. Finally, the stabilization of the product of the reaction is reached by a second protonation of nitrogen in C3 and the concomitant deionization of oxygen in C1.

Table 5: The calculated activation energies (ΔE), enthalpies (ΔH), and Gibbs free energies (ΔG). All values in kcal·mol^{-1}.

	R1	**R2**	**$\Delta E^{\ddagger}$**	**$\Delta H^{\ddagger}$**	**$\Delta G^{\ddagger}$**
1	H	H	1.53	1.16	12.16
2	H	CH_3	7.54	7.12	17.92
3	OH	H	0.54	0.25	11.57

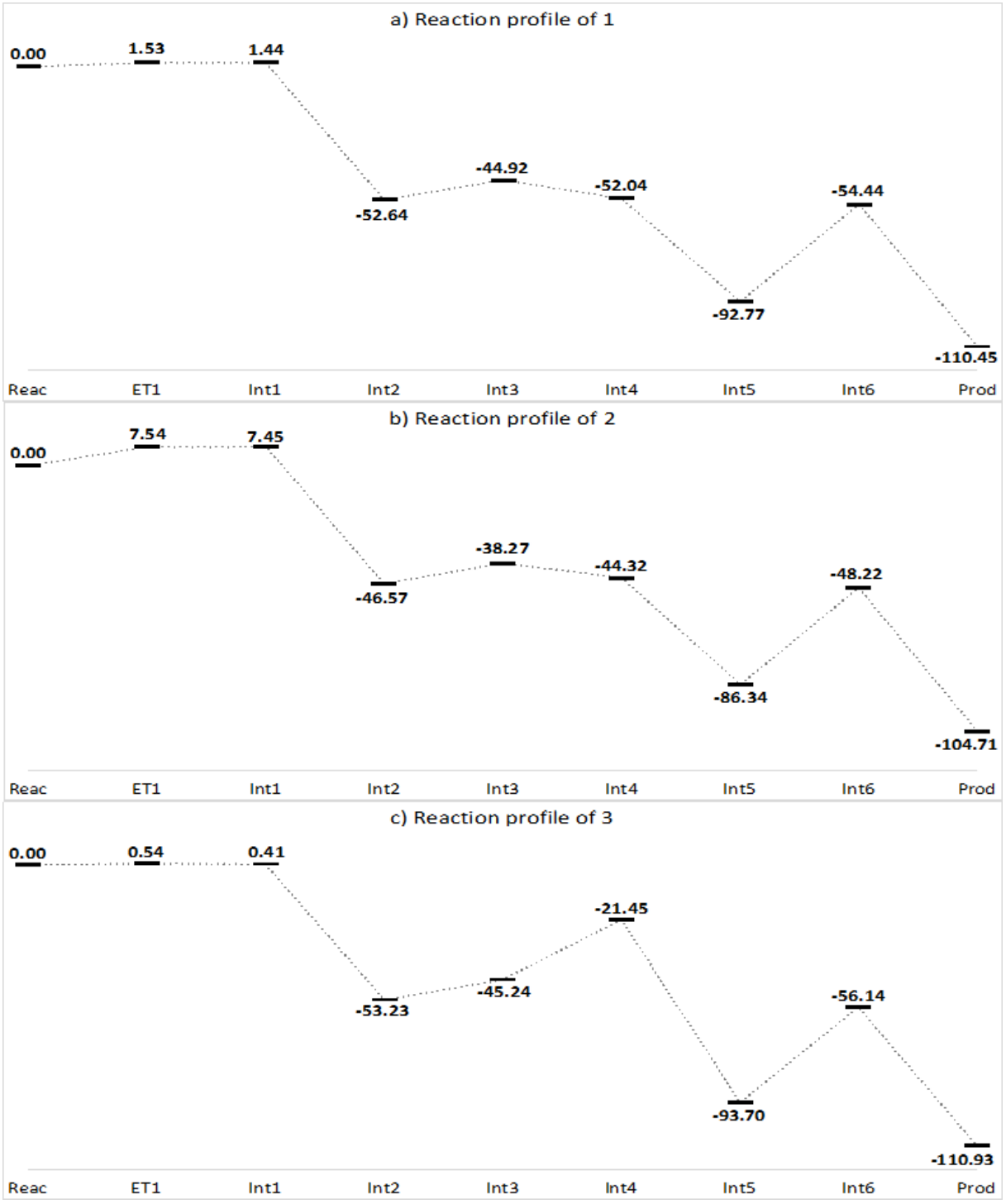

Figure 3: Calculated reaction profile of amination of a) compound **1**, b) compound **2**, and c) compound **3**, based on the minimum energy path at the B3LYP level of calculation.

In Figure 3 are depicted the reaction profile of amination of compounds **1**-**3**. Except for Int1, all intermediates are strongly stable with respect to reactants (the energy

differences are larger than 21 kcal·mol^{-1}), in agreement with a highly favorable reaction and the fact that the nucleophilic addition of N_3^- is the rate determining step of the reaction. Besides, the formation of six intermediates is in line with the extensive time demand of the reaction in the absence of a catalyst.

Conclusion

In summary, compounds **4**-**6** were obtained by amination with hydrazoic acid in the presence of ceric ammonium nitrate. CAN decreases reaction times in the synthesis of compounds, and its molar ratio influences the reaction yield, an excess of catalyst could direct oxidation reactions generating undesirable products. The amination reaction was possible at room temperature except for compound **5**, in which the steric effect of the methyl group on C3 would increase the activation energy. Compound **6** was obtained through a regioselective nucleophilic substitution reaction at C3 promoted by the hydroxyl group at C5 and Cerium. Overall, this kind of reactions are proton aided processes which is speeded up by the presence of cerium atoms of the CAN.

Additionally, a computational study about the reaction mechanism of the amination of naphthoquinones has been carried out. In the reaction energies and enthalpies estimations have been found values higher than 100 kcal·mol^{-1}, favoring the product formation. These values are in agreement with an exothermic and irreversible reaction. Furthermore, the calculated vibrational frequencies enabled identifying the main functional groups, including amino, hydroxyl, and methyl, in line with the experimental characterization of products. Finally, by exploring different reaction pathways, a reaction mechanism has been proposed. The mechanism consists of combining addition and elimination reactions, starting with the nucleophilic addition of the azide

fragment as a rate determining step of the reaction. Subsequently, a sequence of proton additions and eliminations lead to the formation of the aminonaphthoquinone.

Experimental

General Information

All the reagents were ACS grade and purchased from Sigma-Aldrich (St. Louis, MO, USA); the solvents and the Silica 60-230, analytical and preparative thin layer (TLC) chromatography plates were obtained from (Merck Millipore, Billerica, MA, USA). Melting points were measured with a Fisher/Johns melting point apparatus (Thermo Fisher Scientific, Waltham, MA, USA) and were uncorrected. The IR spectra were determined on an FTIR-8400S spectrometer (Shimadzu Corporation, Kyoto, Japan) using KBr disks. The NMR spectra were acquired on Bruker spectrometers (600MHz) (Bruker, Billerica, MA, USA and Bruker, Rheinstetten, Germany) using deuterated acetone and DMSO as a solvent and tetramethylsilane (TMS) as an internal standard. The mass spectra were obtained from an Agilent HP 6890 gas chromatograph equipped with an HP 5973 selective mass detector (Agilent Technologies, Santa Clara, CA, USA). TLC, MS, NMR, and HPLC analytical data confirmed that the purity of test compounds was ≥96%.

Synthesis of 2-amino-1,4-naphthoquinone (4).

To a solution of 1 g of **1** in 50 mL of ethanol was added 2.37 g of sodium azide in 30 mL of distilled water, then was added 3.5 g of CAN, the pH adjusted to 4 with HCl and allowed to stir for 6 h at room temperature. After completing the reaction time, extraction was performed with ethyl acetate (3 X 50 mL). The organic extracts were washed with saline solution, dried over anhydrous Na_2SO_4, and concentrated. The residue was crystallized from methanol to afford an orange needles; 47.6 % yield; m.p.

205 - 207 ºC; FTIR (KBr) √: 3444.59, 3301.59, 3081.74, 2914.92, 2831.03,1686.47, 1607.40 cm^{-1}; ^{1}H-NMR (600 MHz, acetone): δ 8.01 (m, 2H), 7.77 (m, 2H), 6.62 (s, 2H), 5.97 (s, 1H) ppm; ^{13}C-NMR (151 MHz, acetone): δ 182.20 (C4), 182.01 (C1), 149.88 (C2), 134.34 (C7), 133.55 (C9), 131.93 (C6), 130.79 (C10), 125.62 (C8), 125.40 (C5), 103.30 (C3) ppm; MS m/z 173 [M^{+}, $C_{10}H_7O_2N$].

Synthesis of 2-amino-3-methyl-1,4-naphthoquinone (5).

Compound **5** was obtained with the same procedure for the synthesis of **4**, using 2-methyl-1,4-naphthoquinone as starting material and 16 h for reaction time. This afforded a red needles; 65.9% yield; m.p. 158 ºC; FTIR (KBr) √: 3455.87, 3343.05, 2862.85, 1664.29, 1645.87, 11623.79 cm^{-1}; ^{1}H-NMR (600 MHz, acetone): δ 8.04 – 7.96 (m, 2H), 7.78 – 7.66 (m, 2H), 6.12 (s, 2H), 2.01 (s, 3H) ppm; ^{13}C-NMR (151 MHz, acetone): δ 181.64 (C-4), 181.188 (C1), 146.29 (C2), 134.03 (C7), 133.36 (C9), 131.83 (C6), 130.64 (C10), 125.59 (C8), 125.28 (C5), 111.67 (C3), 8.52 (C11) ppm; MS m/z 187 [M^{+}, $C_{11}H_9O_2N$].

Synthesis of 3-amino-5-hydroxy-1,4-naphthoquinone (6).

Compound **6** was obtained with the same procedure for the synthesis of **4**, using 5-hydroxy-1,4-naphthoquinone as starting material and 15 h for reaction time. This afforded a brown needles; 34.6% yield; m.p. >250 ºC; FTIR (KBr) √: 3394.72, 2956.87, 2924.09, 2852.72, 1732.08, 1714.72, 1585.49, 1556.55 cm^{-1}; ^{1}H-NMR (600 MHz, DMSO-d_6): δ 11.49 (s, 1H), 7.68 (m, 1H), 7,42 (m, 1H), 7,18 (m, 1H), 5.77 (s, 1H) ppm; ^{13}C-NMR (151 MHz, DMSO-d_6): δ 186.60 (C1), 181.52 (C4), 160.74 (C5), 150.71 (C3), 137.84 (C7), 133.92 (C9), 122.18 (C8), 117.94 (C6), 114.64 (C10), 102.98 (C2) ppm; MS m/z 189 [M^{+}, $C_{10}H_7O_3N$].

Computational Details

The geometry optimization of compounds **1**-**6** was performed at the B3LYP level of theory [24] with the Ahlrichs def2-TZVP basis set (the resolution of identity approach has been used with the def2/J and def2-TZVP/C auxiliary basis sets for Coulomb and correlation integral calculations, respectively) [25–27], as implemented in the ORCA 4.2.0 package [28,29]. It has also been included the dispersion correction developed by Grimme (included in ORCA by the D3BJ approximation) and the implicit solvent effects by the Conductor-like Polarizable Continuum Model (CPCM) [30]. The dielectric constants and refractive index used for ethanol as a solvent is 24.30 and 1.361, respectively. The threshold for the energy convergence in the self-consistent field procedure was $1x10^{-8}$ a.u. No negative normal modes were obtained by analytical frequency calculations on the optimized geometries. The orca_mapspc module [31] and Avogadro visualization tools have been used for plotting IR spectra and geometries, respectively [32].

Supporting Information

Supporting information features a chromatogram photo of the reaction product of compounds **4**, comparative of theoretical and experimental IR spectra of compounds **4**-**6**, copies of ^{1}H and ^{13}C NMR spectra of compounds **4**-**6**, HMQC and HMBC spectra of compound **6**,

Supporting Information File 1:

File Name: S1.pdf

File Format: PDF

Title: Chromatographic profile of amination reactions of **1** with different molar ratios of CAN.

Supporting Information File 2:

File Name: S2.pdf

File Format: PDF

Title: Theoretical IR spectra of compounds **4**-**6**

Supporting Information File 3:

File Name: S3.pdf

File Format: PDF

Title: ^{1}H and ^{13}C NMR spectra of compounds **4**-**6**

Supporting Information File 4:

File Name: S4.pdf

File Format: PDF

Title: HSQC and HMBC spectra of compounds **6**

Acknowledgments

We acknowledge Prof. Marisa Cabeza from Autonomous Metropolitan University-Xochimilco for helpful assistance as a tutor in the international internship. J. Z. R. also acknowledges the access to the computational facilities of HPC provided by Universidad de los Andes.

Funding

The following funding sources are acknowledged: Vice-rectory for research at the University of Cartagena for financing the research project approved by resolution

02007 of 2018, and Universidad de los Andes through the project FAPA PR.3.2019.6668.

References

1. Babula, P.; Adam, V.; Havel, L.; Kizek, R. *Curr. Pharm. Anal.* **2009**, *5*, 47–68.
2. Durán, A. G.; Chinchilla, N.; Molinillo, J. M. G.; Macías, F. A. *Pest Manag. Sci.* **2019**, *75*, 2517–2529.
3. Widhalm, J. R.; Rhodes, D. *Hortic. Res.* **2016**, *3*, 1–17.
4. Gaitan, R.; Arguello, E.; Alvarez, W.; Jaraba, S.; Martelo, J.; Zambrano, R.; Diaz, F.; Hernandez, A. *Rev. Cuba. Química* **2007**, *XIX*, 64–66.
5. Jali, R.; Behura, R.; Barik, R.; Parveen, S.; Mohanty, P.; Das, R. *Res. J. Pharm. Technol.* **2018**, *11*, 3698–3702.
6. Perry, N.; Blunt, J.; Munro, M. *J. Nat. Prod.* **1991**, *54*, 978–985.
7. Epifano, F.; Genovese, S.; Fiorito, S.; Mathieu, V.; Kiss, R. *Phytochem. Rev.* **2014**, *13*, 37–49.
8. Celio, G.; Rocha, F.; Miqueias, L.; Luciana, F.; Roy, K.; Doerksen, R.; Braga, A.; Rocha, G. *Eur. J. Med. Chem.* **2018**, *145*.
9. Dong, M.; Liu, D.; Li, Y.; Chen, X.-Q.; Luo, K.; Zhang, Y.-M.; Li, R.-T. *Planta Med.* **2017**, *83*, 631–635.
10. Rengasamy, G.; Hussain, S.; Balakrishna, J.; Rex, J.; Suga, S.; Ravikumar, D.; Sivagnanam, P. *J. Crit. Rev.* **2020**, *7*, 1216–1238.
11. Kutyrev, A. A. *Tetrahedron* **1991**, *47*, 8043–8065.
12. Yamashita, M. Y.; Eda, K. U.; Sakaguchi, K. S.; Tokuda, H. T.; Iida, A. I. **2011**, *59*, 1289–1293.
13. Gholampour, M.; Ranjbar, S.; Edraki, N.; Mohabbati, M.; Firuzi, O.;

Khoshneviszadeh, M. *Bioorg. Chem.* **2019**, *88*, 102967.

14. Suja, T. D.; Divya, K. V. L.; Naik, L. V.; Ravi Kumar, A.; Kamal, A. *Bioorganic Med. Chem. Lett.* **2016**, *26*, 2072–2076.
15. Nawrat, C. C.; Palmer, L. I.; Blake, A. J.; Moody, C. J. *J. Org. Chem.* **2013**, *78*, 5587–5603.
16. Fieser, L.; Hartwell, L. *J. Am. Chem. Soc.* **1935**, *57*, 1482–1484.
17. Couladouros, E. A.; Plyta, Z. F.; Haroutounian, S. A.; Papageorgiou, V. P. *J. Org. Chem.* **1997**, *62*, 6–10.
18. Acuña, J.; Piermattey, J.; Caro, D.; Bannwitz, S.; Barrios, L.; López, J.; Ocampo, Y.; Vivas-Reyes, R.; Aristizábal, F.; Gaitán, R.; Müller, K.; Franco, L. *Molecules* **2018**, *23*, 1–21.
19. Andrade-guel, M. L. *TIP Rev. Espec. en Ciencias Químico-Biológicas* **2011**, *14*, 75–82.
20. Macias, M.; López, L.; Sáenz, A.; Silva, S. *Rev. Científica la Univ. Autónoma Coahuila* **2013**, *5*, 20–26.
21. Bittner, S.; Lempert, D. *Synthesis (Stuttg).* **1994**, *1994*, 917–919.
22. Arnone, A.; Merlini, L.; Nasini, G.; Pava, O. V. De. *Synth. Commun.* **2007**, *37*, 2569–2577.
23. Karaman, R. *Comput. Theor. Chem.* **2011**, *974*, 133–142.
24. Stephens, P. J.; Devlin, F. J.; Chabalowski, C. F.; Frisch, M. J. *J. Phys. Chem.* **1994**, *98*, 11623–11627.
25. Weigend, F.; Ahlrichs, R. *Phys. Chem. Chem. Phys.* **2005**, *7*, 3297–3305.
26. Weigend, F. *Phys. Chem. Chem. Phys.* **2006**, *8*, 1057–1065.
27. Hellweg, A.; Hättig, C.; Höfener, S.; Klopper, W. *Theor. Chem. Acc.* **2007**, *117*, 587–597.
28. Neese, F. *Wiley Interdiscip. Rev.-Comput. Mol. Sci* **2012**, *2*, 73–78.

29. Neese, F. *Wiley Interdiscip. Rev. Comput. Mol. Sci.* **2018**, *8*, 1–6.

30. Grimme, S.; Ehrlich, S.; Goerigk, L. *J. Comput. Chem.* **2011**, *32*, 1456–1465.

31. Petrenko, T.; George, D.; Aliaga-alcalde, N.; Bill, E. *J. Am. Chem. Soc.* **2007**, *129*, 11053–11060.

32. Hanwell, M. D.; Curtis, D. E.; Lonie, D. C.; Vandermeersch, T.; Zurek, E.; Hutchison, G. R. *J. Cheminform.* **2012**, *4*, 1–17.